

Splice variants of the P2X7 receptor reveal differential agonist dependence and functional coupling with pannexin-1

Xing Jian Xu¹, Miyyada Boumechache¹, Lucy E. Robinson¹, Viola Marschall¹, Dariusz C. Gorecki², Marianela Masin¹ and Ruth D. Murrell-Lagnado^{1,*}

¹Department of Pharmacology, University of Cambridge, Tennis Court Road, Cambridge CB2 1PD, UK

²School of Pharmacy and Biomedical Sciences, University of Portsmouth, White Swan Road, Portsmouth PO1 2DT, UK

*Author for correspondence (rdm1003@cam.ac.uk)

Accepted 18 April 2012

Journal of Cell Science 125, 3776–3789

© 2012. Published by The Company of Biologists Ltd

doi: 10.1242/jcs.099374

Summary

P2X7 receptors function as ATP-gated cation channels but also interact with other proteins as part of a larger signalling complex to mediate a variety of downstream responses that are dependent upon the cell type in which they are expressed. Receptor-mediated membrane permeabilization to large molecules precedes the induction of cell death, but remains poorly understood. The mechanisms that underlie differential sensitivity to NAD are also unknown. By studying alternative variants of the mouse P2X7 receptor we show that sensitivity to NAD is mediated through the P2X7k variant, which has a much more restricted distribution than the P2X7a receptor, but is expressed in T lymphocytes. The altered N-terminus and TM1 of the P2X7k receptor enhances the stability of the active state of this variant compared with P2X7a, thereby increasing the efficacy of NAD-dependent ADP ribosylation as measured by ethidium uptake, a rise in intracellular Ca^{2+} and the activation of inward currents. Co-expression of P2X7k and P2X7a receptors reduced NAD sensitivity. P2X7k-receptor-mediated ethidium uptake was also triggered by much lower BzATP concentrations and was insensitive to the P451L single nucleotide polymorphism. P2X7k-receptor-mediated ethidium uptake occurred independently of pannexin-1 suggesting a pathway intrinsic to the receptor. Only for the P2X7aL451 receptor could we resolve a component of dye uptake dependent upon pannexin-1. Signalling occurred downstream of the activation of caspases rather than involving direct cross talk between the channels. However, an *in situ* proximity assay showed close association between P2X7 receptors and pannexin-1, which would facilitate ATP efflux through pannexin-1 acting in an autocrine manner.

Key words: NAD, P2X7, Pannexin

Introduction

P2X7 receptors are predominantly immune and epithelial cell receptors which mediate many diverse responses that include the processing and release of proinflammatory cytokines, the phagocytosis and subsequent killing of pathogens, increased cell proliferation and survival and cell death by apoptosis and necrosis (Adinolfi et al., 2005; Brough et al., 2002; Cabrini et al., 2005; Chen and Brosnan, 2006; Di Virgilio et al., 2001; Guerra et al., 2003; Mackenzie et al., 2005; North, 2002; Placido et al., 2006). They have low affinity for extracellular ATP compared to the other members of the P2X family (North, 2002) and the levels required to maximally stimulate the receptor are more likely to occur where there is pathology or injury; thus it has been postulated that this receptor mediates the actions of ATP as a danger signal. The role of this receptor in diseases that involve chronic inflammation or cancer makes it a potentially useful therapeutic target, and antagonists have been developed and tested for clinical trials (Chessell et al., 2005; Dardano et al., 2009; Donnelly-Roberts and Jarvis, 2007; Feng et al., 2006a; Wiley et al., 2002).

How the expression and activation of P2X7 receptors triggers such a diversity of responses is not well understood. Similar to other P2X receptors, when activated they mediate the rapid flux of mono- and divalent cation, and the resulting loss of K^+ from the cell and

rise in Ca^{2+} are both involved in triggering downstream responses (North, 2002). What distinguishes the P2X7 receptor from the other members of this family is its very long cytoplasmic C-terminal tail, which is important for targeting of this receptor to the plasma membrane, its function and for interactions with other proteins (Denlinger et al., 2001; Kim et al., 2001; North, 2002; Nuttle and Dubyak, 1994; Smart et al., 2003; Wilson et al., 2002). This region confers upon the receptor additional unique functions that distinguish it from the other P2X subtypes. One of the most extensively studied is membrane permeabilization to relatively large molecules up to 900Da in size that occurs within seconds of activating the P2X7 receptor and is routinely assayed by the uptake of fluorescent dyes such as ethidium (North, 2002; Nuttle and Dubyak, 1994). This process occurs on a similar time scale to receptor-triggered externalization of phosphatidylserine (PS) to the plasma membrane outer leaflet and precedes membrane blebbing (Mackenzie et al., 2005; Pfeiffer et al., 2004; Verhoef et al., 2003). These responses are associated with P2X7 receptor dependent cell death, and single nucleotide polymorphisms (SNPs) that inhibit the large pore formation, similarly inhibit cell death. One such SNP is P451L; this substitution occurs naturally in the C57BL/6 strain of mice and reduces the rate of dye uptake but does not compromise agonist-evoked whole-cell currents (Adriouch et al., 2002; Le Stunff et al., 2004).

The P2X7 receptor is thought to exist as part of a larger signalling complex, and several proteins have been identified as interacting with it. These include cytoskeletal elements and other ion channels including the P2X4 receptor and pannexin-1 (Boumechache et al., 2009; Denlinger et al., 2001; Gu et al., 2009; Iglesias et al., 2008; Kim et al., 2001; Pelegrin and Surprenant, 2006). The interaction between P2X7 and pannexin-1 (PANX1) was proposed to play an important role in mediating membrane permeabilization to large molecules with the suggestion that PANX1 forms the large pore rather than it being intrinsic to the P2X7 receptor itself. Overexpression of PANX1 increased the rate of P2X7 receptor-mediated dye uptake whereas knock down of PANX1 function either by siRNA or the use of pharmacological inhibitors reduced dye uptake (Iglesias et al., 2008; Locovei et al., 2006; Pelegrin and Surprenant, 2006). PANX1 channels pass strongly outwardly rectifying currents, provide a route for efflux of ATP and are blocked by carbenoxolone (CBX) and a mimetic peptide (¹⁰panx1) (Scemes et al., 2009). They are activated by caspases, which recognize a site between residues 376 and 379 and cleave the C-terminus (Chekeni et al., 2010). Hypotonic shock is also reported to activate the channel suggesting that it might be mechano-sensitive (Locovei et al., 2006; Ransford et al., 2009).

The proposal that PANX1 is the principal dye-uptake pathway triggered by the activation of the P2X7 receptor remains controversial. There is evidence for two distinct pathways, one for anions and the other for cations, with inhibitors of PANX1 blocking neither pathway (Cankurtaran-Sayar et al., 2009; Schachter et al., 2008). PANX1-mediated currents were shown to be inhibited by ATP and 3'-O-(4-benzoyl)benzoyl ATP (BzATP) at concentrations commonly used to activate P2X7 receptors (Ma et al., 2009; Qiu and Dahl, 2009). Finally, recent experiments using bone marrow derived macrophages from PANX1 deficient mice have shown that dye uptake in these cells is not reduced compared to wild-type cells, suggesting that PANX1 is not required for P2X7 receptor-mediated dye uptake (Qu et al., 2011). An alternative hypothesis is that dye uptake is intrinsic to the P2X7 receptor and in support of this idea is the evidence to indicate that the pore of P2X7, and other P2X subtypes, can dilate during prolonged agonist application. Although initially selective for small mono and divalent cations, over a period of seconds, the permeation of larger cations such as NMDG⁺ is permitted (Eickhorst et al., 2002; Khakh et al., 1999; Virginio et al., 1999; Yan et al., 2008).

The cellular responses triggered by the P2X7 receptor will depend upon the structure of the receptor itself in addition to the expression of other proteins with which it can interact. Several splice variants and SNPs have been identified for both the human and rodent isoforms, some of which are linked with disease (Adriouch et al., 2002; Cabrini et al., 2005; Cheewatrakoolpong et al., 2005; Dardano et al., 2009; Feng et al., 2006a; Gu et al., 2001; Nicke et al., 2009). For the human receptor, a prevalent C-terminal truncated splice variant, P2X7B, has been described which fails to trigger membrane permeabilization to large molecules but still stimulates the rate of cell growth (Adinolfi et al., 2010; Cheewatrakoolpong et al., 2005). We have described similar C-terminal truncated variants of the mouse isoform (Masin et al., 2012), plus a novel rodent splice variant, P2X7k, which utilizes an alternative exon 1 encoding the N-terminus and part of the TM1. The rat P2X7k receptor is activated by lower agonist concentrations than the P2X7a variant and shows faster kinetics of membrane permeabilization and blebbing; properties

that are more consistent with the cell death promoting actions of P2X7 receptor signalling (Nicke et al., 2009).

Variation in P2X7 receptor structure could explain the differential sensitivity to agonist displayed by receptors expressed in different cell types. P2X7 receptors in mouse T-lymphocytes are activated by nicotinamide adenine dinucleotide (NAD) in addition to ATP, whereas macrophage P2X7 receptors are not (Hong et al., 2009; Seman et al., 2003). NAD is a substrate for ADP ribosylation of the receptor, a reaction that is catalyzed by ART2.2, a GPI-anchored ADP-ribosyltransferase (Adriouch et al., 2008). Micromolar levels of NAD triggers phosphatidylserine flip and ultimately cell death of T-lymphocytes (Seman et al., 2003). In contrast, macrophages show no response despite expressing ART2.1 (Hong et al., 2009).

In this study we investigated the contribution of the P2X7a and P2X7k receptor variants to the diversity of P2X7 receptor signalling and also took advantage of the differences in their properties to probe the nature of the functional coupling between P2X7 and PANX1 and the role PANX1 plays in receptor-mediated membrane permeabilization. We show that the P2X7k receptor variant is responsible for NAD-dependent gating of the T-cell receptors and provide evidence for the formation of P2X7a/k heteromers with reduced sensitivity to agonist. Rapid dye uptake triggered by P2X7k receptor activation is independent of PANX1 and only when dye uptake is compromised in the P2X7a variant can a PANX1 dependent component be resolved, downstream of caspase activation.

Results

Enhanced sensitivity of the P2X7k receptor and tolerance of the L451 SNP

We compared the functional properties of the mouse P2X7a and k receptor variants with the expectation that the enhanced activity of the k variant that was previously shown for the rat isoform (Nicke et al., 2009) would also be seen when comparing the mouse receptors. We did this using the two backgrounds, P451 and L451, to test whether or not leucine at position 451 impairs dye uptake in the more active k variant as was shown for the P2X7a receptor (Adriouch et al., 2002). Whole-cell currents measured in HEK cells heterologously expressing the two receptors indicated that BzATP was more potent at the P2X7k than the P2X7a receptor (Fig. 1A). Concentration–response relationships were generated by normalizing currents for each cell to the response to 1 mM and 100 μM BzATP for the P2X7a and P2X7k receptors respectively. The EC₅₀ values were ~10-fold lower for the P2X7k versus P2X7a receptor but the curves overlapped for the L451 and P451 forms. Comparing peak current densities, the responses evoked by 300 μM BzATP were considerably larger for the P2X7k receptor compared to the P2X7a receptor (Fig. 1B), but when responses to doses close to the EC₅₀ values and near maximal were compared, there was no significant difference in the peak current densities between all 4 forms of the receptor. Thus, functional plasma membrane expression of the receptors appears to be similar.

Membrane permeabilization to fluorescent dyes was measured by confocal microscopy. For the P2X7a receptor, L451 reduced the rate of BzATP-stimulated ethidium uptake compared to P451, as shown previously (Adriouch et al., 2002), whereas for the P2X7k receptor there was no compromise in ethidium uptake for L451 compared to P451 (Fig. 1C). Concentration–response curves were generated by subtracting the constitutive rate of

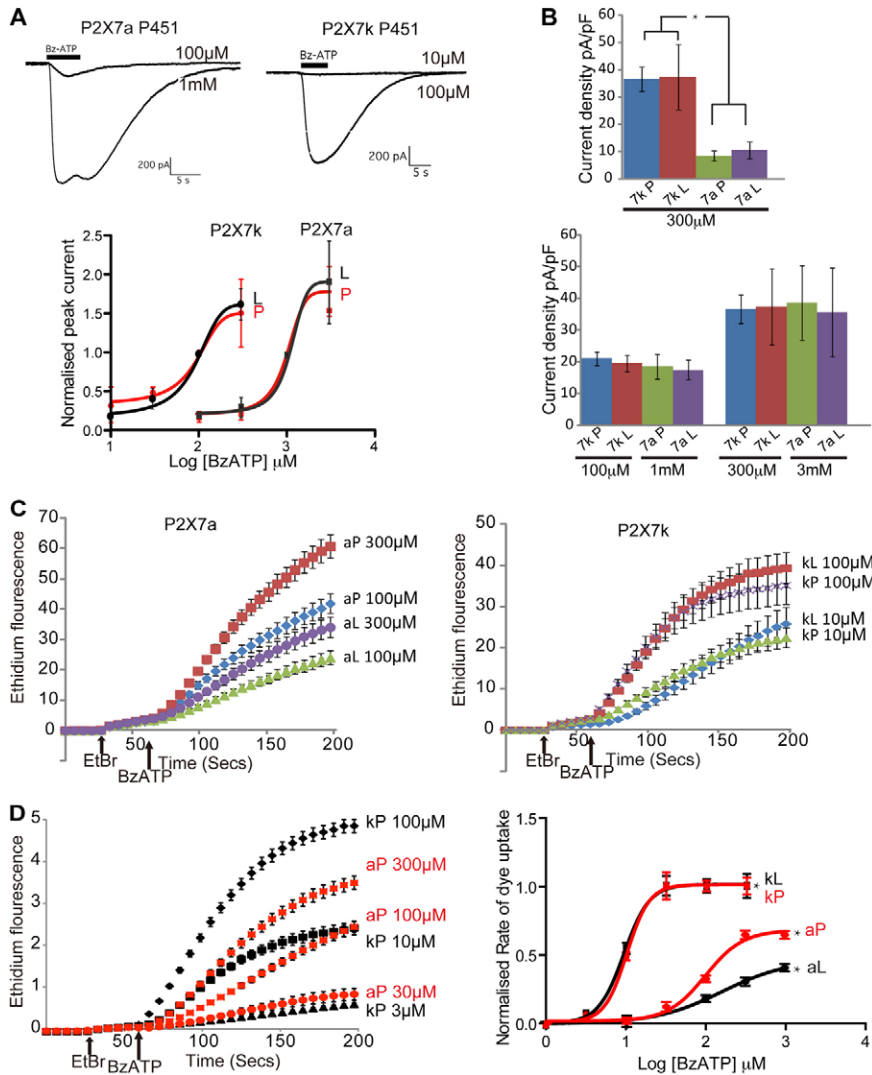


Fig. 1. The P2X7k receptor variant is activated by lower agonist concentrations and mediates dye uptake insensitive to the P451L SNP. (A) Whole-cell patch-clamp recordings from HEK cells expressing either the P2X7k or P2X7a receptor, with P451.

Currents were evoked by a 5 s application of BzATP at a holding potential of -60 mV. To generate concentration–response curves, currents in each cell were normalized to the response to either 1 mM BzATP, for P2X7a, or 100 μ M BzATP, for the P2X7k receptor. EC₅₀ values: P2X7aL, 1.1 mM; P2X7aP, 1.0 mM; P2X7kL, 125 μ M; P2X7kP, 105 μ M ($n=4-6$ cells).

(B) The current densities evoked by 300 μ M BzATP show the significantly larger responses at the P2X7k versus P2X7a receptors ($n=4-6$ cells; $*P<0.01$). Comparing responses to doses close to the EC₅₀ values and near maximal, the current densities were very similar for all four forms of the receptor.

(C) Representative time courses of the increase in fluorescence, as measured by confocal microscopy, in HEK cells expressing either P2X7a or P2X7k receptors following application of BzATP at the concentrations stated, in the presence of ethidium bromide (20 μ M). The P451L SNP reduced dye uptake mediated by P2X7a but not P2X7k receptors.

(D) A comparison of the rate of ethidium uptake mediated by P2X7aP and P2X7kP receptors. Concentration–response curves for the rate of increase in fluorescence 15–35 s following BzATP application, normalized to the rate mediated by P2X7kP in response to 100 μ M BzATP, measured on the same day. Recordings were made in a low divalent extracellular solution. EC₅₀ values: P2X7aL, 147 μ M; P2X7aP, 100 μ M; P2X7kL 9.93 μ M; P2X7kP, 10.2 μ M ($n=3$ with 60 cells analyzed per experiment).

Comparing the maximal rate of dye uptake mediated by the receptors, there was a significant difference between P2X7k and P2X7a receptors ($*P<0.01$) and between P2X7aP and P2X7aL receptors ($*P<0.01$).

ethidium uptake from the rate of uptake 15–35 s post application of BzATP, and normalizing to the response to 100 μ M BzATP at the P2X7kP receptor (Fig. 1D). For the P2X7k receptor the EC₅₀ values were again at least tenfold lower than for the P2X7a receptor and the maximal response was also significantly higher ($P<0.01$). The EC₅₀ values were reduced compared to the current measurements because experiments were carried out in the low divalent extracellular solution. Interpreting these results, for the P2X7a receptor, the selective effect of the P451L mutation on dye uptake indicates that there are at least two distinct active states, one that permits the flux of small cations and the other that also, directly or indirectly, permits influx of the cationic dye, ethidium. The permissive state for dye influx does not appear to be a higher conducting state for the major charge carrying ion, Na⁺. For the P2X7k receptors both active states are more stable and not compromised by the leucine at position 451.

P2X7k receptor is expressed in splenic T lymphocytes and mediates the effects of NAD

Previously, we showed that the P2X7k receptor is expressed in the spleen of the Glaxo P2X7^{-/-} mice but not in bone marrow derived macrophages from these mice, nor in many other tissues

(Boumechache et al., 2009; Nicke et al., 2009). To determine whether or not T lymphocytes in the spleen express this receptor we isolated them from freshly dissociated tissue and probed for expression of P2X7 using a C-terminal antibody. A band of the expected size was detected in T-lymphocytes from both WT and P2X7^{-/-} mice (Fig. 2A). Although we cannot distinguish between P2X7a and P2X7k receptors in the WT tissue, expression of P2X7a receptors is abolished in the P2X7^{-/-} mice and therefore we are confident that the receptor detected here represents P2X7k.

T-cell P2X7 receptors can be activated by NAD via ADP ribosylation catalyzed by ART2 (Seman et al., 2003). Macrophage receptors and P2X7a receptors co-expressed with ART2.2 in HEK cells are insensitive to NAD (Hong et al., 2009). To investigate the possibility that P2X7k receptors mediates NAD sensitivity we co-expressed P2X7kP451 with ART2.2 in HEK cells and measured ethidium uptake over a range of NAD concentrations up to 300 μ M. Concentrations of NAD of 10 μ M and above stimulated ethidium uptake compared to the rate observed in the absence of NAD and the effect was dependent upon the co-expression of ART2.2 (Fig. 2B). The potentiation by NAD was all-or-nothing over the time scale of these experiments

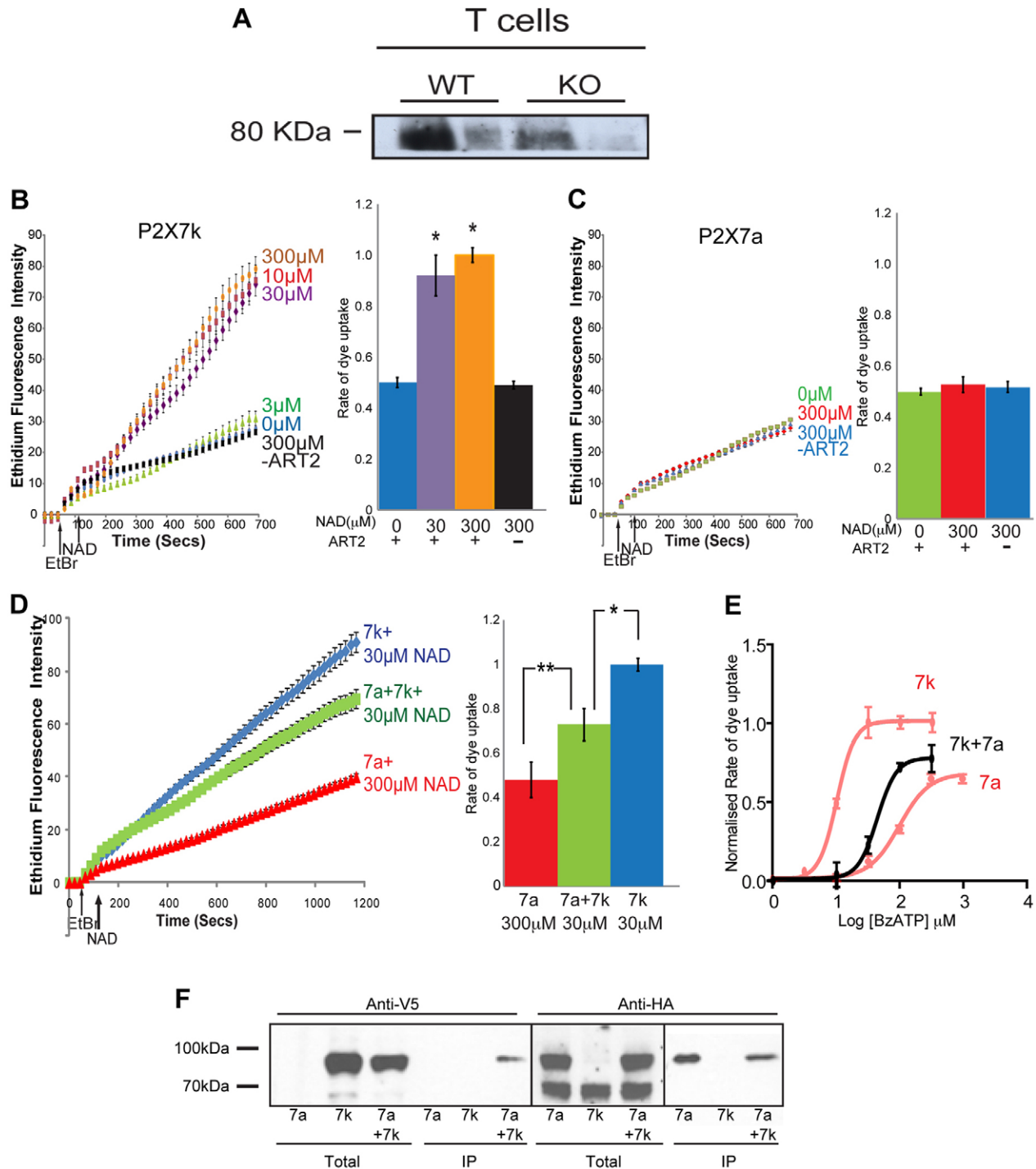


Fig. 2. P2X7k receptor is expressed in splenic T lymphocytes and mediates dye uptake in response to NAD-stimulated ADP ribosylation. (A) Western blot of T lymphocytes isolated from the spleen of WT mice and Glaxo P2X7^{-/-} mice. Two dilutions from each sample were run and P2X7 was detected using a C-terminal anti-P2X7 antibody that detects both P2X7a and P2X7k receptors. (B) NAD-stimulated increase in ethidium fluorescence in cells co-expressing the P2X7kP(451) receptor and ART2.2 or P2X7kP alone. Ethidium bromide was added at 60 s and NAD at 120 s. The rate of increase in fluorescence (between 30–100 s after NAD addition) was significantly greater following application of either 30 μ M or 300 μ M NAD than in the absence of NAD or in cells that did not co-express ART2.2 ($n=80$ –180 cells; $*P<0.01$). (C) HEK cells co-expressing P2X7aP receptors and ART2.2 or P2X7aP alone did not respond to NAD ($n=60$ –130 cells; $P>0.05$). (D) For HEK cells co-expressing both P2X7aP and P2X7kP receptors with ART2.2, the rate of increase in fluorescence following application of 30 μ M NAD was significantly less than in cells expressing P2X7kP receptors alone ($n=80$ –120 cells; $P<0.01$), but greater than in cells expressing P2X7aP receptors alone (** $n=80$ –130 cells; $P<0.05$). (E) The concentration–response relationship for BzATP-stimulated ethidium uptake for cells co-expressing P2X7a and P2X7k receptors, normalized to the response mediated by P2X7k receptors expressed alone (100 μ M). Recordings were made in low divalent NES ($EC_{50} = 44$ μ M; $n=3$; 60 cells per experiment). (F) Western blot analysis using the anti-V5 antibody (left) and anti-HA antibody (right) showed P2X7k–V5 was co-immunoprecipitated with P2X7a–HA using the anti-HA resin, but only when the receptors were co-expressed.

with 3 μM having no effect and 10 μM producing a similar increase in dye uptake as the higher doses. At the P2X7aP451 receptor, NAD over a similar range of concentrations had no effect on the rate of ethidium uptake either with or without ART2.2 (Fig. 2C). The co-expression of P2X7a and P2X7k receptors reduced the response to NAD compared to cells expressing P2X7k alone, suggesting that these two variants form heteromers with reduced sensitivity (Fig. 2D). The BzATP concentration–response curve for the co-expressed receptors was intermediate between the two receptors expressed individually (Fig. 2E). These results are consistent with the observations of Taylor et al., who showed that T cells from the Glaxo P2X7^{-/-} mice which lacked P2X7a receptors, were more responsive to ATP than T cells from the WT mice, suggesting that P2X7k homomeric receptors are more active than the P2X7a/k heteromers (Taylor et al., 2009).

To further investigate a structural interaction between P2X7a and P2X7k subunits we differentially tagged them at the C-terminus with an HA and V5 epitope, respectively. Following expression in HEK cells, purification was carried out using an anti-HA resin followed by elution from the resin using an HA peptide. A band of the expected size for P2X7a-HA was detected in the immunoprecipitate when P2X7a-HA was expressed alone or together with P2X7k-V5, whereas P2X7k-V5 was only co-immunoprecipitated when P2X7a-HA was present (Fig. 2F). This indicates an interaction between the two subunits consistent with the formation of heteromeric receptors. The expression of P2X7a-HA was very similar when expressed alone or together with P2X7k-V5 although there was a slight decrease in P2X7k-V5 expression when co-expressed with P2X7a-HA. This would not, however, explain the shift in the concentration–response relationship if receptors were functioning independently of one another.

NAD-dependent ADP ribosylation acts as a partial agonist at P2X7k receptors

To further characterize the effects of NAD on both P2X7a and k receptors we measured changes in $[\text{Ca}^{2+}]_i$ and whole-cell currents in HEK cells expressing these receptors with ART2.2. Changes in $[\text{Ca}^{2+}]_i$ were measured using Fura-Red and confocal microscopy and in cells expressing P2X7k receptors there was a clear and sustained increase in $[\text{Ca}^{2+}]_i$ following application of 30 μM NAD, whereas there was no response to 300 μM NAD in cells expressing P2X7a receptors (Fig. 3A). Whole cell patch clamp of P2X7k receptor expressing cells showed an inward current evoked by 300 μM NAD with activation kinetics slower than BzATP-evoked currents and no clear deactivation of the current following wash out of NAD, over the time period of these experiments (1–2 min) (Fig. 3B). The amplitude of NAD-evoked currents was much smaller than currents activated by a near maximal dose of BzATP. For cells expressing the P2X7a receptor there was no inward current activated by 300 μM NAD, however cells exposed to NAD for 5 s gave a smaller response to a subsequent application of 3 mM MgATP compared to cells only exposed to ATP (Fig. 3C) and the extent of the inhibition was dependent upon the concentration of NAD. Similarly, for P2X7k receptors, prior exposure to 30 μM NAD for 5 s, did not evoke a current but reduced the response to subsequent application of 1 mM MgATP. The inhibitory effects of NAD on dye uptake mediated by BzATP were also observed for both receptors (Fig. 3D). These results suggest that both P2X7a and P2X7k

receptors are ADP ribosylated by application of NAD and that whilst this acts as a partial agonist at P2X7k receptors, it acts as an antagonist at P2X7a receptors. These results are broadly consistent with those of Hong et al., who showed that P2X7a receptors were ADP ribosylated by NAD application but that this failed to trigger a rise in $[\text{Ca}^{2+}]_i$ unless there was a R276K gain of function mutation in the receptor (Hong et al., 2009).

Differential effects of PANX1 expression on P2X7a- and P2X7k-receptor-mediated ethidium uptake seen with the L451 SNP

Both active states of the P2X7k receptor are more stable than for the P2X7a receptor; BzATP is more potent, ADP ribosylation is more efficacious and the P451L substitution is no longer sufficient to impair activity with respect to ethidium uptake. To investigate the mechanism underlying the rapid ethidium uptake mediated by P2X7k receptors we looked at the role of PANX1 channels. HEK cells stably overexpressing an HA-tagged version of the human isoform of PANX1 were generated (PANX1-HEK) and immunostaining with anti-HA showed expression of the channel at the plasma membrane whilst western blot analysis of proteins treated with either N-glycosidase F (F-Gnase), to remove all glycans, or endoglycosidase H, to remove only simple glycans, showed that the hemichannel was complex glycosylated and thus not retained within the endoplasmic reticulum (Fig. 4A,B). A comparison of constitutive ethidium uptake in the PANX1-HEKs versus WT HEKs showed that in the majority of PANX1-HEKs there was no enhancement in the rate of dye uptake compared to the untransfected cells, but that there was a small population of PANX1-HEKs showing elevated ethidium uptake (Fig. 4C), which might correspond to cells that have higher levels of caspase activity. To further test the functionality and pharmacology of PANX1 channels we measured dye uptake in response to a hypotonic stimulus, previously shown to activate these channels. There was a modest increase in rate but this was not significantly reduced by carbenoxolone (CBX), a known inhibitor of PANX1 (Fig. 4D). We next compared whole-cell currents activated by hypotonic shock in WT and PANX1-HEK cells. Hypotonic shock activated a strongly outwardly rectifying current in the PANX1-HEKs that was of much larger amplitude than the WT HEKs (Fig. 4E). This hypotonic-shock-induced current was abolished by pretreatment with either CBX or the ¹⁰panx1 mimetic peptide (Fig. 4F,G). It was also inhibited by transfecting siRNA targeted against hPANX1 into these cells (Fig. 4H). Finally we co-expressed P2X7a receptors in the PANX1-HEKs and this also significantly reduced the amplitude of hypotonic-shock-induced outward currents, suggesting that the receptor in its closed state exerts an inhibitory effect on PANX1 channel activation (Fig. 4I).

As a measure of colocalization between co-expressed P2X7 receptors and PANX1 channels we used an in situ proximity ligation assay in combination with the anti-HA antibody, to recognize PANX1-HA, and an anti-P2X7 C-terminal antibody. The hPANX1 is 94% identical with the mouse isoform at the amino acid level (Baranova et al., 2004). There was a strong positive signal for P2X7 with PANX1, whereas neither P2X4 nor P2X2 expressed in these cells with their relevant antibodies gave any signal to indicate proximity with PANX1 (supplementary material Fig. S1A). Although P2X7 colocalized with PANX1, enhanced expression of the hemi-channel did not affect surface trafficking of

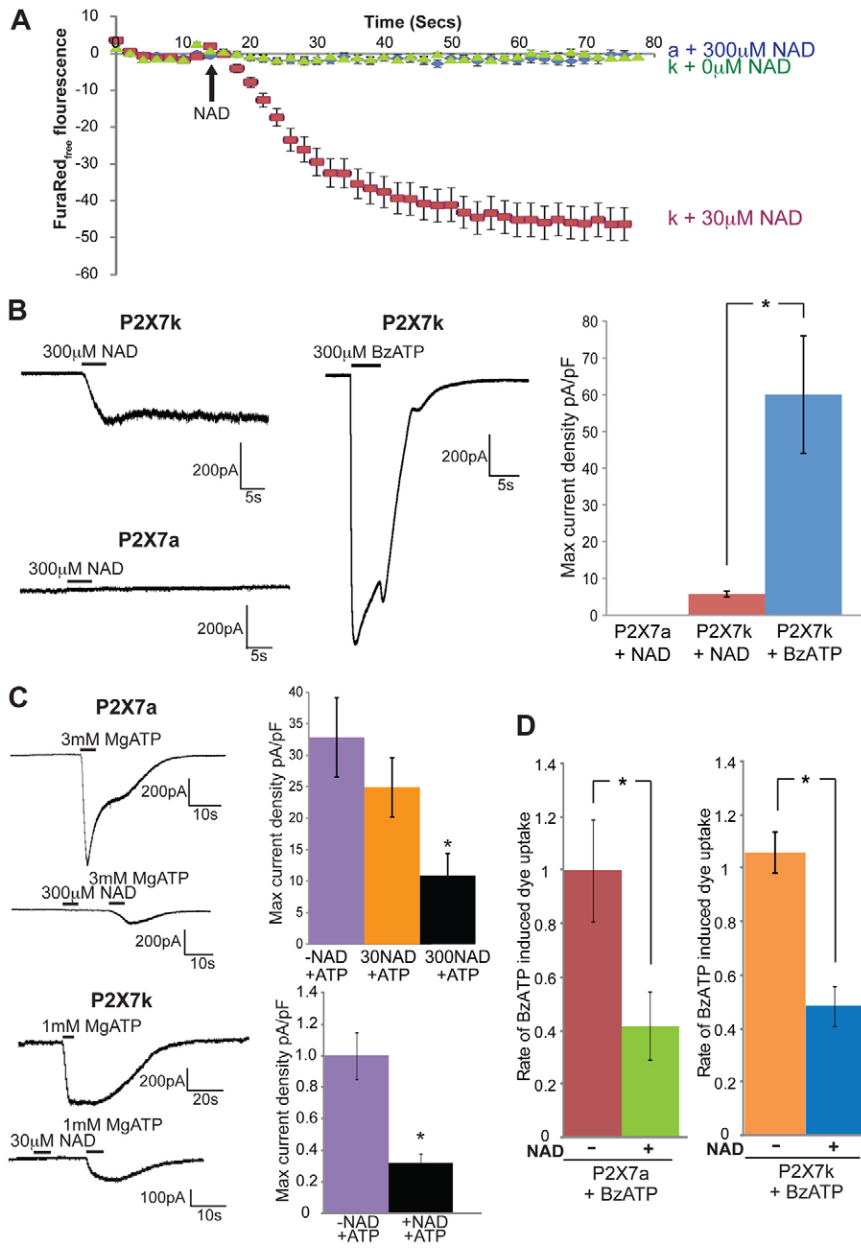


Fig. 3. Differential effects of NAD-dependent ADP ribosylation on P2X7k and P2X7a receptor-mediated responses. (A) The time course of NAD-induced rise in cytosolic free Ca^{2+} in HEK cells co-expressing P2X7aP451 or P2X7kP451 receptors with ART2.2 measured by confocal microscopy using the Ca^{2+} -sensitive indicator Fura-Red. A decrease in fluorescence indicates a rise in free $[\text{Ca}^{2+}]_i$. Cells were incubated in 6 μM Fura-Red for 30 min at 37 $^{\circ}\text{C}$ prior to imaging. (B) Whole-cell patch-clamp recordings from cells expressing either P2X7kP or P2X7aP receptors with ART2.2, in response to a 5 s application of NAD or BzATP. P2X7a receptors did not respond to NAD. The histogram summarizes the mean peak current densities and shows the significant difference between NAD- and BzATP-evoked responses ($P < 0.01$, $n = 5-8$). (C) Despite P2X7a receptors not responding to NAD, prior application of NAD (5 s) reduced their response to subsequent application of MgATP (3 mM, 5 s) in a dose-dependent manner. There was a 10 s wash between the NAD and the MgATP applications. Summary histogram shows that the mean peak current density was significantly reduced after a 5 s exposure to 300 μM NAD ($n = 4-7$ cells; $*P < 0.01$). Similarly, a 5 s exposure to 30 μM NAD, reduced the response of P2X7k receptors to a subsequent dose of MgATP ($n = 4-7$ cells; $*P < 0.01$). (D) The rate of ethidium uptake mediated by P2X7aP and P2X7kP receptors in response to 300 μM and 100 μM BzATP, respectively, was also significantly reduced by the application of 300 μM NAD 20 s prior to the addition of BzATP. P2X7a: $n = 65-80$ cells; $*P < 0.01$. P2X7k: $n = 65-85$ cells; $*P < 0.01$.

the receptor, as indicated either by the biotinylation and purification of surface proteins or by the use of a membrane impermeable cross linker BS³, which linked only subunits within receptors exposed at the cell surface (supplementary material Fig. S1B).

Having shown enhanced expression of functional PANX1 channels in the stably transfected cells we compared ethidium uptake triggered by P2X7aL451 and P2X7aP451 receptors in both WT and PANX1-HEK cells in response to 300 μM BzATP. For the P451 receptor the rate of ethidium uptake in WT and PANX1-HEK cells was very similar, whereas for the L451 receptor the rate of uptake in WT cells was $\sim 25\%$ of the rate for the P451 receptor, but this increased approximately threefold in the PANX1-HEKs (Fig. 5A). To determine if sensitivity to PANX1 expression is conferred by the L451 residue, we tested ethidium uptake mediated by P2X7kL451 receptor in response to 100 μM BzATP. For this variant there was no significant

difference between WT and PANX1-HEK cells and the rate was more than fourfold faster than for the P2X7aP451 receptor (Fig. 5B). Similar experiments were performed but using a low-dose of BzATP (10 μM and 30 μM) to partially activate P2X7kL451 and P2X7aP451 receptors. Although the rates of ethidium uptake were much slower, again there was no difference between PANX1-HEKs and WT HEKs (Fig. 5C). Consistent with these observations, CBX had no effect on the rate of dye uptake mediated by either of these receptors in PANX1-HEKs, indicating that the PANX1 channels were not involved in this process. For the P2X7aL451 receptor, however, the increase in ethidium uptake seen in the PANX1-HEKs was blocked by treatment with either CBX or the ¹⁰panx1 inhibitory peptide (Fig. 5D). Increased ethidium uptake is therefore mediated via the overexpressed PANX1 channels. We also tested the effects of an inhibitor of caspase-dependent apoptosis, zVAD-fmk, because

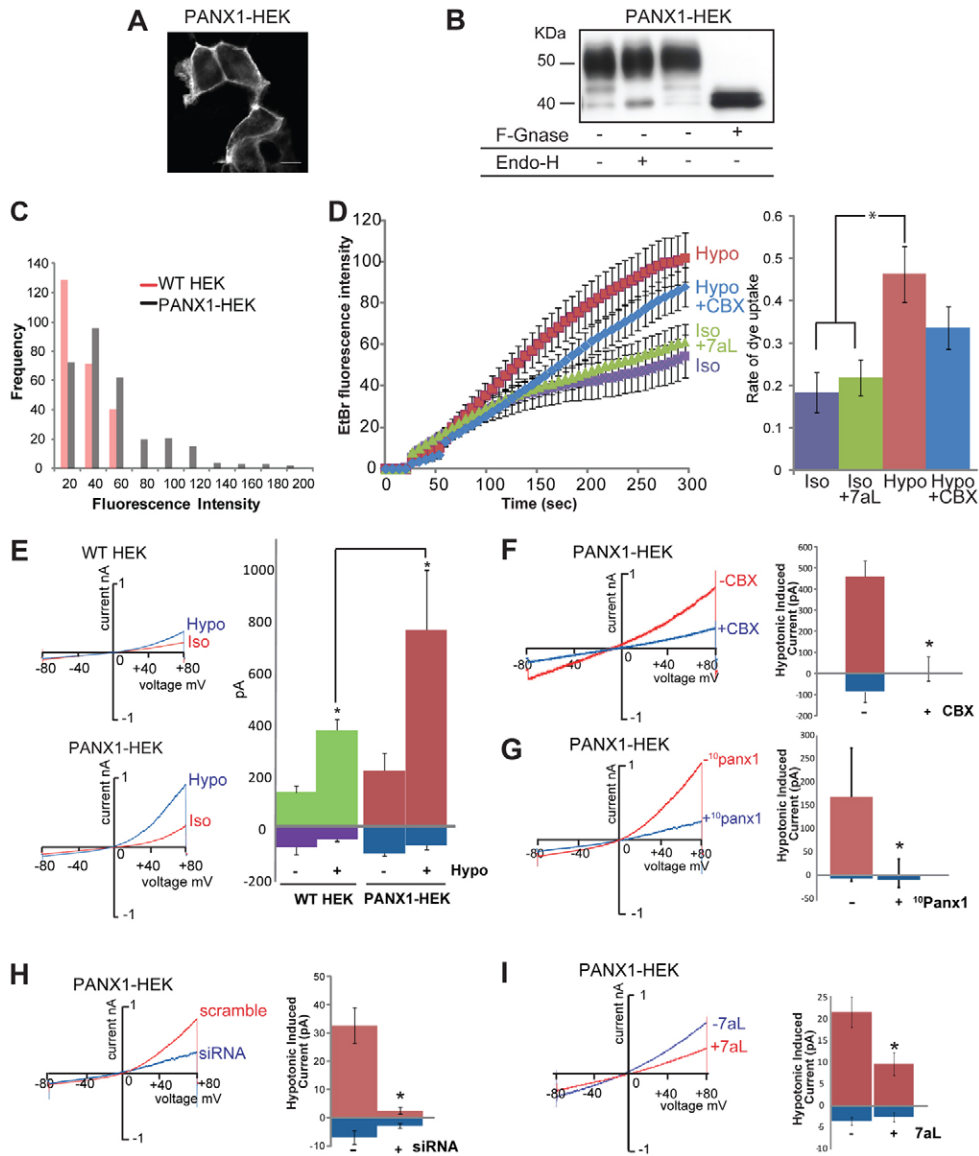


Fig. 4. Analysis of PANX1 channel function in HEK293 cells stably over-expressing the human isoform shows activation by hypotonic stimulus. (A) hPANX1-HA was stably expressed in HEK cells (PANX1-HEK) and immunostaining with anti-HA antibody showed that the protein was expressed at the plasma membrane. Scale bar: 10 μ m. (B) Western blot using the anti-HA antibody of protein samples from PANX1-HEKs subjected to de-glycosylation treatments shows that the majority of PANX1-HA protein was resistant to EndoH, indicating that it was complex glycosylated in the trans-Golgi network. (C) Frequency histogram comparing constitutive ethidium uptake in WT and PANX1-HEK cells following incubation with ethidium bromide in isotonic NES for 10 min at room temperature. Dye uptake was enhanced in a small proportion ($\sim 20\%$) of the PANX1-HEKs ($n=250-300$ cells). (D) Co-expression of the P2X7aL receptor in PANX1-HEKs did not affect the rate of constitutive ethidium uptake. There was, however, a small but significant increase in the rate of ethidium uptake in hypotonic solution ($n=40-50$; $*P<0.05$) and this was reduced in the presence of 100 μ M carbenoxolone (CBX) but not significantly ($n=40-50$; $P>0.05$). (E) Whole-cell patch-clamp recordings from WT HEK cells and PANX1-HEKs showed that hypotonic shock induced a much larger strongly outward-rectifying current in the PANX1-HEKs. The voltage was ramped between -80 mV and $+80$ mV. Hypotonic shock was applied by replacing the isotonic NES (290 mOsm/l) with hypotonic NES (190 mOsm/l). The histogram shows the mean current amplitudes at -80 mV and $+80$ mV before and after hypotonic shock ($n=6-8$; $*P<0.05$). (F) Similar experiments were carried out to show that in the presence of 100 μ M CBX, the hypotonic-shock-induced current in PANX1-HEKs was dramatically reduced ($n=6$; $P<0.01$). (G) Pre-incubation of PANX1-HEKs with 100 μ M ¹⁰panx1 peptide for 15 min at 37°C, significantly reduced the hypotonic-shock-induced current ($n=5$; $P<0.05$). (H) Transfection of PANX1-HEKs with siRNA targeted against hPANX1 significantly reduced the hypotonic-shock-induced response compared with scrambled siRNA ($n=4$; $P<0.01$). (I) Co-expression of P2X7aL451 receptors in the PANX1-HEKs significantly reduced the amplitude of hypotonic-shock-induced currents ($n=4$; $P<0.05$).

caspace-dependent cleavage of PANX1 can directly activate the channel and P2X7 receptor activation promotes apoptosis. Pre-incubation with zVAD-fmk reduced P2X7aL451-mediated dye uptake in the PANX1-HEKs to a level similar to that seen in the

presence of the PANX1 inhibitors. This suggests that signalling between P2X7aL451 and PANX1 occurs downstream of the activation of caspases. When we tested the effects of the PANX1 antagonists on receptor-mediated dye uptake in WT HEKs there

was no inhibition for either P2X7aL451 (Fig. 5E) or P2X7k receptors (Fig. 5F). Dependency on PANX1 is thus restricted to the condition in which the receptor with impaired ethidium

uptake (P2X7aL451) is co-expressed with the recombinant PANX1 channels and the increase in dye uptake occurs over a range of agonist concentrations (Fig. 5G).

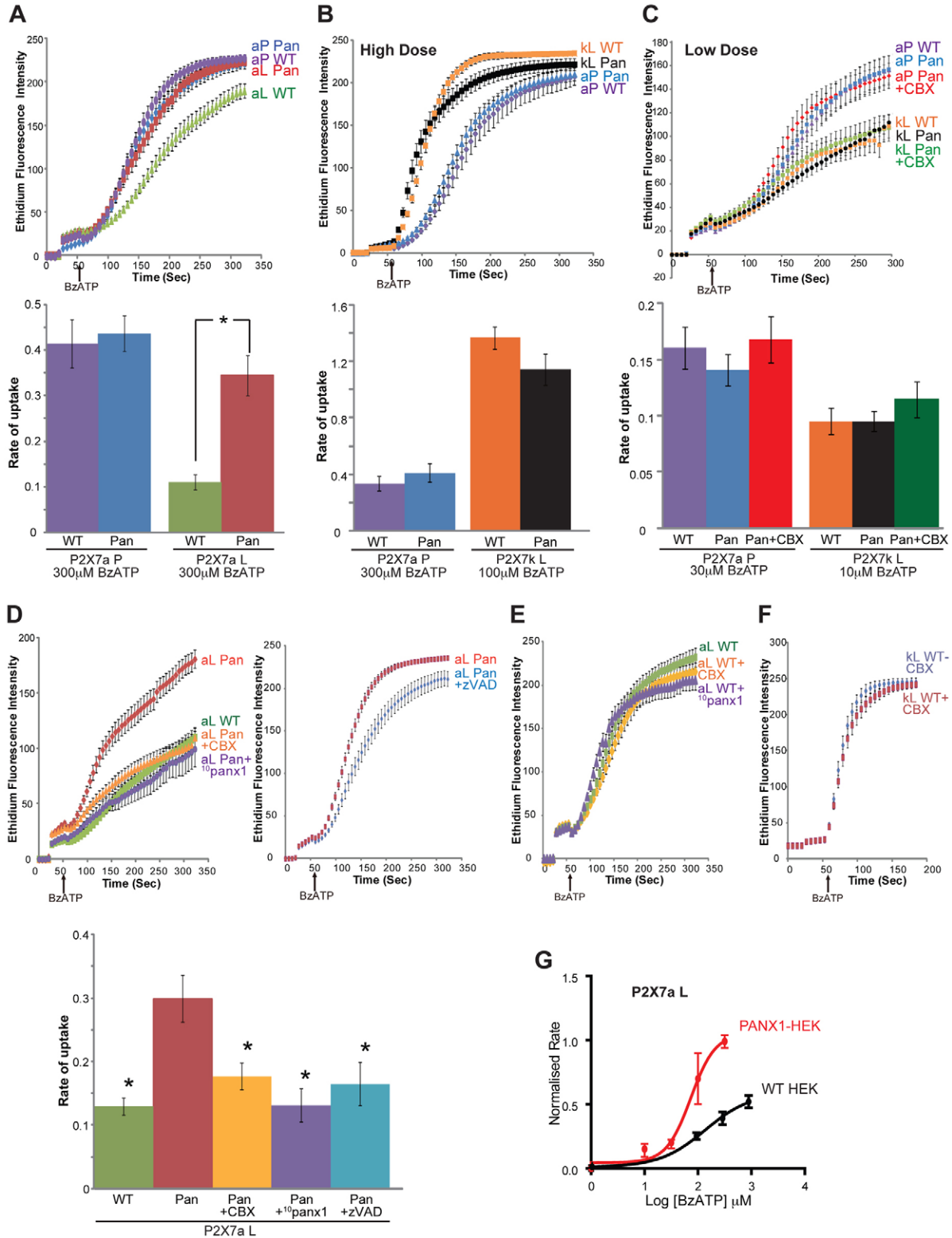


Fig. 5. See next page for legend.

Knockdown of PANX1 expression had no effect on ethidium uptake mediated by P2X7a or P2X7k receptors with P451

To further investigate coupling between PANX1 channels and the P2X7 receptors we inhibited PANX1 expression using siRNA. The efficiency of knockdown was tested in the PANX1-HEKs where we could use the anti-HA antibody to compare expression levels (Fig. 6A). In three separate experiments, western blot analysis suggested that expression was reduced by between 50–80%. Immunostaining also showed effective knockdown following transfection with siRNA (Fig. 6B). Comparison of ethidium uptake in WT HEK cells co-transfected with the different P2X7 receptor variants and either PANX1 siRNA or scrambled siRNA showed no difference in the rate of ethidium uptake following PANX1 knockdown, consistent with the lack of effect of CBX in these cells (Fig. 6C). In contrast, when PANX1-HEKs were co-transfected with PANX1 siRNA and P2X7aL451 there was a significant reduction in the rate of dye uptake compared to the scrambled siRNA condition (Fig. 6D). The effect of the PANX1 siRNA was similar to the inhibitory effects of CBX and zVAD-fmk and there was no additivity between siRNA and CBX treatment and between zVAD-fmk and CBX, consistent with them all acting by effectively abolishing PANX1 function.

Discussion

The comparison of the functional properties of the mouse P2X7a and k receptors indicates that the k variant expressed in T-lymphocytes is responsible for the NAD-dependent activation of P2X7 receptors. Although both receptors are targets for ART2.2-mediated ADP ribosylation, this modification is more efficacious for the P2X7k variant and acts as a partial agonist of the receptor, whereas at P2X7a it elicits no response. ADP ribosylation permitted both the flux of small cations and the uptake of

ethidium mediated via the P2X7k receptor. The stabilization of the active states of P2X7k compared to the P2X7a receptor is also reflected in the increased potency of BzATP and insensitivity to the P451L SNP. Despite the close proximity of coexpressed P2X7 and PANX1 channels, P2X7 receptors mediate rapid uptake of ethidium independently of PANX1 and only for the P2X7aL451 receptor, which shows reduced uptake, did we resolve a PANX1 component to ethidium uptake when the hemichannel was overexpressed. This coupling was mediated exclusively via caspase activation, rather than direct cross-talk between the channels, as indicated by the inhibitory effects of zVAD-fmk and the lack of any additivity when CBX was used in combination with zVAD-fmk. These results show splice variants of the rodent P2X7 receptor contributing to cell-type-dependent diversity of P2X7 receptor function and provide evidence that they can function as homo- and heteromers. They also suggest that ethidium uptake, in addition to the transport of small cations, is an intrinsic property of the receptor itself.

The restricted distribution of the P2X7k receptor

Previous analysis of the distribution of the P2X7k variant indicated that it has a much more restricted expression than the P2X7a variant (Nicke et al., 2009). Although the transcript for P2X7k was identified in all of the wild type mouse tissue tested, when we analyzed expression of the protein in the Glaxo P2X7^{-/-} mice, the only tissue with clear expression was the spleen (Boumechache et al., 2009; Nicke et al., 2009). The ability of the P2X7k receptor to escape inactivation in the Glaxo P2X7^{-/-} mice is because the disruption to the gene occurs in the original exon 1 that is not utilized in the k variant. We were unable to analyze expression of P2X7k protein in WT mice because the antibodies available to us do not discriminate between the two variants. The restricted distribution of P2X7k receptors explains why the NAD sensitivity of endogenous P2X7 receptors has only been reported in T-lymphocytes.

ADP ribosylation acting as a partial agonist

Our finding that the P2X7a receptor co-expressed with ART2.2 in HEK cells is unresponsive to NAD even at high concentrations has been shown previously (Adriouch et al., 2008). Gain-of-function mutations were identified within the extracellular loop of the receptor that promote NAD-dependent gating. They also identified R125 as the target for ADP ribosylation and proposed that the adenine nucleotide moiety fits into the ligand-binding pocket of P2X7 between two adjacent subunits. Presumably this modification would prevent the binding of soluble ATP within the same pocket, which is consistent with our finding that NAD can antagonize the actions of BzATP at the P2X7a receptor. The identification of the P2X7k receptor as the mediator of the T-cell NAD responses is important because this splice variant is restricted to rodents and there is no human equivalent (Nicke et al., 2009). In mice, NAD is an important physiological regulator of T-cell P2X7 receptors because the concentration of NAD required to activate these receptors is much lower than for ATP; in the micromolar rather than the millimolar range. The release of NAD by lytic and non-lytic mechanisms during inflammation causes shedding of CD62L, PS flip and ultimately cell death (Seman et al., 2003). Regulation of human T cells by NAD is however likely to differ. Our prediction is that at the hP2X7a receptor, NAD will have two actions: to antagonize the effects of high doses of ATP, similar to what we have shown for

Fig. 5. P2X7aL451 receptor shows a pannexin-1-dependent component of dye uptake but the other variants do not. (A) Representative time course of 300 μ M BzATP-activated ethidium uptake for P2X7aL451 and P2X7aP451 receptors in WT HEK (WT) and PANX1-HEK cells (Pan). Summary histogram compares the mean rate of increase in fluorescence between 15–35 s after application of BzATP and shows that uptake in PANX1-HEK compared to WT cells was significantly greater for P2X7aL, but not for P2X7aP receptors ($n=6$, 60 cells per experiment; $*P<0.01$). (B) A similar experiment, this time comparing dye uptake mediated by the P2X7kL receptor with that of the P2X7aP receptor, shows the much faster rate for P2X7kL and no affect of over-expression of PANX1. (C) The lack of dependence on PANX1 for P2X7aP and P2X7k receptors was also seen at lower doses of BzATP (10 μ M and 30 μ M for P2X7kL and P2X7aP, respectively). Consistent with this there was no effect of 100 μ M CBX on the rate of ethidium uptake in PANX1-HEK cells. (D) For P2X7aL, the potentiation of ethidium uptake in the PANX1-HEKs was abolished in the presence of inhibitors, CBX (100 μ M) and the ¹⁰panx1 peptide (100 μ M). Pre-incubation with zVAD-fmk (5 μ M, 60 min at 37°C) also reduced ethidium uptake in the PANX1-HEKs. The summary histogram is shown below ($n=3$, 60 cells per experiment; $*P<0.05$, comparing all conditions to the PANX1-HEKs). (E) In contrast to the PANX1-HEKs, ethidium uptake mediated by P2X7aL in WT HEK cells was insensitive to CBX and ¹⁰panx1 peptide. (F) Similar results were obtained for P2X7k receptors in WT HEKs. (G) Concentration–response relationship for P2X7aL451 receptors activated by BzATP in WT HEK cells and PANX1-HEK cells shows the increased rate of ethidium uptake over a range of concentrations (PANX1-HEK cells: EC₅₀=75 μ M; WT HEK cells, EC₅₀=147 μ M; $n=3$, 60 cells per experiment).

mP2X7a receptors, but at low doses of ATP, to act synergistically. Hong et al. showed that at mP2X7a receptors, pre-stimulation with 100 μ M NAD for 3–5 mins decreased the threshold concentration of ATP required to activate a P2X7

receptor-mediated rise in $[Ca^{2+}]_i$ (Hong et al., 2009). With at least two ATP molecules required to bind to fully activate the receptor an explanation for this result is that if a significant proportion of receptors are only partially occupied with ATP,

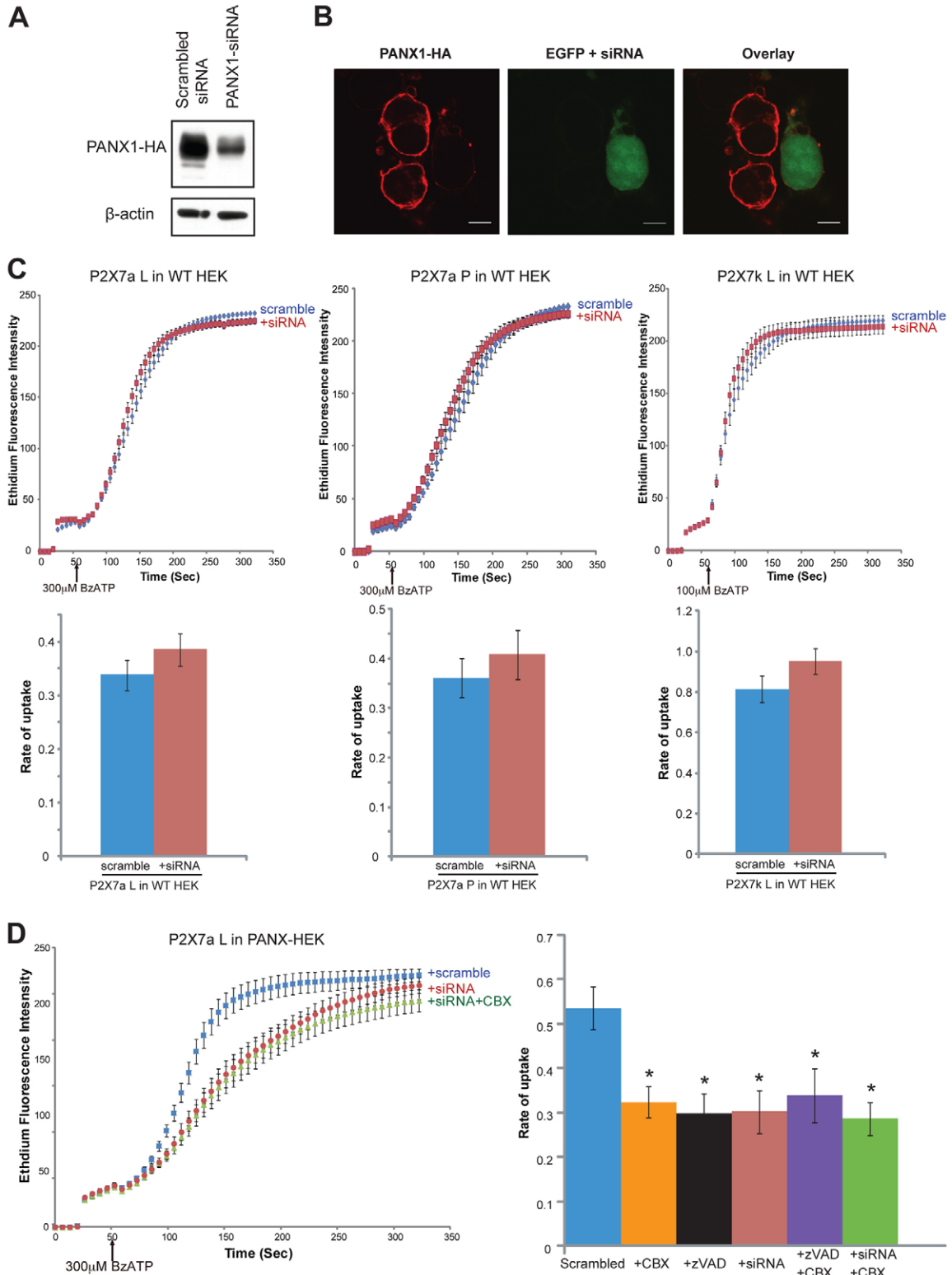


Fig. 6. See next page for legend.

then ADP ribosylation at the other site(s) might be sufficient to promote activity. It is also possible that other variants of the hP2X7 receptor are expressed in human T lymphocytes. Many splice variants of the hP2X7 primary transcript have been identified (Cheewatrakoolpong et al., 2005), the most prevalent being the hP2X7b variant which has a very large deletion at the C-terminus. This receptor has reduced function compared to the hP2X7a receptor, does not trigger membrane permeabilization to large molecules and thus seems an unlikely candidate for mediating the effects of NAD (Adinolfi et al., 2010; Cheewatrakoolpong et al., 2005). Also analysis of the expression of mRNA for hP2X7b showed expression in the spleen and T lymphocytes, but at a lower level than for the P2X7a mRNA. Other variants of the hP2X7 receptor have been shown to be non-functional (Feng et al., 2006b).

An intrinsic pathway for cation dye influx

The results of our experiments involving PANX1 overexpression and knockdown are inconsistent with some previous studies, which reported a crucial role for PANX1 in the P2X7 receptor-mediated dye-uptake process in HEK cells (Iglesias et al., 2008; Locovei et al., 2007; Pelegrin and Surprenant, 2006; Pelegrin and Surprenant, 2009). Others, however, have also failed to demonstrate an important role for PANX1 (Faria et al., 2005; Schachter et al., 2008; Taylor et al., 2008). Our findings argue in favour of the receptor itself forming an intrinsic pathway for the influx of cationic dyes. One argument against an intrinsic pathway for dye uptake is based upon the identification of a proximal C-terminal region of P2X7 that appears to differentially control permeability to NMDG⁺ and dyes (Jiang et al., 2005). Deletion of this region of 18 amino acids (Y358–E375) in rat P2X7 was reported to inhibit permeability to NMDG⁺ without inhibiting receptor-mediated dye uptake suggesting the involvement of two different pathways. A later study with human P2X7, however, showed that this same deletion caused the receptor to be instantaneously permeable to NMDG⁺ upon opening rather than inhibiting permeability (Yan et al., 2008). The ability to dissociate NMDG⁺ and dye permeation, does not, however, provide conclusive evidence for the involvement of two different proteins. If NMDG⁺ and ethidium do utilize a similar

pathway, then interactions between these cations and the receptor are likely to differ and thus be differentially sensitive to site-directed mutagenesis.

Functional coupling between P2X7 receptors and PANX1

Despite concluding that cationic dye uptake is intrinsic to the receptor we were able to characterize a PANX1-dependent component of receptor-mediated ethidium uptake, under conditions where the intrinsic pathway was compromised by the P451L substitution and PANX1 expression was high. Thus we were able to demonstrate that signalling between P2X7 receptors and PANX1 occurs downstream of the activation of caspases. Our inability to resolve the PANX1 component under other conditions is probably because it was considerably slower than the intrinsic pathway. In some cellular context, however, the PANX1 pathway might play a significant role in P2X7 receptor-mediated membrane permeabilization, dependent upon the expression levels of the two proteins, the duration and extent to which the receptor is activated and the presence of interacting partners that might compromise intrinsic dye uptake, as has been suggested for the interaction between P2X7 receptor and non-muscle myosin IIA (Gu et al., 2009). We also showed an inhibitory effect of P2X7 receptor expression on hypotonic-shock-induced PANX1 activity, consistent with functional coupling between the two channels, and close proximity between P2X7 receptors and PANX1 when they are co-expressed. This could help to ensure that PANX1-mediated release of ATP promotes the activation of P2X7 in an autocrine manner. In Jurkat T cells, PANX1-mediated ATP efflux is triggered by apoptosis (Chekeni et al., 2010) and in erythrocytes and retinal ganglion cells, PANX-mediated ATP efflux is triggered by hypotonic stress (Bao et al., 2004; Locovei et al., 2006). The autocrine action of ATP released from human T cells has been shown to be an important mechanism for regulating endogenous P2X7 responses. The activation of the T-cell receptor causes the rapid release of ATP, which acts back upon the cells to stimulate P2X7 receptors thereby triggering a rise in [Ca²⁺]_i, NFAT activation and interleukin-2 production (Yip et al., 2009). A role for PANX1 in this process, however, has not yet been identified.

Materials and Methods

All reagents were purchased from Sigma Chemical Co. Ltd (UK) unless otherwise stated. Culture media were supplied by GIBCO (UK). Endoglycosidase H (EndoH) and N-glycosidase F (F-Gnase) kits were purchased from Roche (UK) and New England Biolabs (UK), respectively, and used according to manufacturers' instructions. Caspase family inhibitor, zVAD-fmk was purchased from BioVision (USA). Mouse anti-V5 antibody was obtained from Invitrogen (UK). Anti-HA mouse monoclonal antibody was obtained from COVANCE (USA) and rabbit polyclonal P2X7 C-terminus (P2X7-CT), P2X2, and P2X4 antibodies from Alomone (Israel). Anti-mouse and anti-rabbit HRP-conjugated secondary antibodies were obtained from ThermoScientific (UK) and BioRad (UK), respectively. The proximal ligation assay kit was from Olink Bioscience (UK). The pannexin-1 mimetic peptide ¹⁰panx1 (WRQAAFVDSY) was synthesized by Cambridge Bioscience (UK). siRNA duplexes were supplied by SigmaGenosys in a powder form and were dissolved in RNase-free water. The solution was then aliquoted and stored at -20°C and used within 3 months. The anti-pannexin-1 siRNA (PANX1-siRNA) sequence (5'-GCAUCAAAUCAGGAUCCU-3') was the same as that used previously (Pelegrin and Surprenant, 2006).

Drugs

All incubations with drugs were conducted at 37°C, 5% CO₂ in a humidified incubator unless otherwise stated. zVAD-fmk was used at a final concentration of 5 μM in DMEM with 60 min pre-incubation with the samples. The ¹⁰panx1 peptide was used at a final concentration of 100 μM in NES with 15 min pre-incubation with the samples. Carbenoxolone (CBX) was used at a final concentration of 100 μM in NES unless otherwise stated.

Fig. 6. Knock-down of PANX1 by siRNA had no effect on P2X7-receptor-mediated ethidium uptake in WT HEKs but reduced uptake mediated by P2X7aL451 receptors in PANX1 cells. Western blot (A) and immunostaining (B) with the anti-HA antibody shows that transfection of PANX1-siRNA markedly reduced the expression of PANX1 in HEK cells stably overexpressing PANX1-HA (PANX1-HEK). Staining with anti-HA used the Cy3 secondary antibody and pEGFP was co-transfected with the PANX1-siRNA to identify transfected cells. In three individual western blot experiments, expression of PANX1-HA was reduced by between 50 and 80% following siRNA transfection. Scale bars: 10 μm. (C) The time courses of BzATP-activated ethidium uptake in WT HEKs co-transfected with P2X7aL, P2X7aP or P2X7kL, with either PANX1-siRNA or scrambled siRNA, shows that there was no effect of PANX1 knockdown in the WT cells (*n*=3). (D) In contrast, BzATP-activated ethidium uptake for P2X7aLeu in PANX1-HEKs was inhibited by co-transfecting PANX1-siRNA. The extent of inhibition was very similar to pre-treatment with zVAD-fmk or CBX (*n*=3; **P*<0.05, comparing all conditions to the scrambled siRNA treatment). There was no additivity between PANX1-siRNA and CBX or between zVAD-fmk and CBX indicating that all treatments effectively abolished PANX1 function.

Animals

Spleen was obtained from adult C57 WT and Glaxo P2X7^{-/-} (Sikora et al., 1999) mice as described previously (Masin et al., 2012). All procedures were performed with permission of the local Animal Health and Welfare Committees and in accordance with the UK Home Office guidelines.

DNA constructs

P2X2, P2X4 and P2X7 were subcloned into the Clontech GFP-N1 vector using the NotI site to excise the coding sequence for GFP (Guo et al., 2007). hPANX1 bearing an HA tag (YPYDVPDYA) at the C-terminus was amplified using the following sense and anti-sense primers: 5'-AGCATAGAAATTCGTGCCACCATATGCGCCATCGCTCAACTGGCC-3' and 5'-TCTATGCGCCGCTTATGCGTAGTCTGGCAGCTCGTATGGGTAGCAAGAAGAATCCAGAAGTCTC-3'.

P2X7a bearing an HA tag at the C-terminus was amplified using the following sense and anti-sense primers: 5'-AGCATAAAGCTTGTGCCACCATGCCGGC-TTGTCGAGCTGG-3' and 5'-GCGAACGCGGCCGCTCATGCGTAGTCTGG-CACGTCGTATGGTACTGAGCCACCATGATGTGGCAGC-3'.

P2X7k bearing a V5 tag at the C-terminus was amplified using the following sense and anti-sense primers: 5'-AGCATAAAGCTTGTGCCACCATGCTGCC-CGTGAGCCACTTATG-3' and 5'-GCGAACGCGGCCGCTCACGTGGAGTC-GAGACCGAGGAGGGTTAGGGATAGGCTTACCCTGAGCCACCATGATGTTGGCAGC-3'.

All constructs were subcloned into the Clontech GFP-N1 vector.

Cell culture

The HEK293 cells were maintained as described previously (Guo et al., 2007; Moore and MacKenzie, 2007). They were routinely transfected using calcium phosphate or Lipofectamine 2000 also as described previously (Guo et al., 2007).

Generation of stable PANX1-HEK cell line

HEK293 cells were seeded in six-well plates and 12–16 hours later, 60–70% confluent cells were transfected with the plasmid encoding hPANX1 using calcium phosphate. After 48 hours post-transfection, geneticin (G418), 0.8 mg/ml in fresh medium, was added to the cells to select for transfected clones and the medium was changed every other day. Once confluent, cells were transferred into flasks and maintained in medium containing G418 (0.8 mg/ml) for a total of 4 weeks from the transfection date.

siRNA transfection

siRNA was transfected into HEK293 cells using Lipofectamine 2000 (Invitrogen). Briefly, 50–60% confluent cells seeded in 6-well plates were incubated in a fresh antibiotic-free medium for at least 2 hours prior to transfection. siRNA (200 pmol) and DNA (1 µg) were diluted in opti-MEM (200 µl) and incubated at room temperature for 5 min. This was combined with Lipofectamine 2000 (6 µl) which was also made up in 200 µl opti-MEM, and left for a further 20 min at room temperature in the dark. The transfection mix was added dropwise to the cells (400 µl/well). The cells were maintained at 37°C and the medium was changed 24 hours later. Experiments were carried out 48 hours post-transfection.

Surface biotinylation, BS³ cross-linking and immunoblotting

Procedures were conducted as described previously (Boumechache et al., 2009).

Co-immunoprecipitation

Transfected cells were washed twice in ice-cold HBS supplemented with 2 mM EDTA, harvested, and the membrane solubilised in HBS containing 1% Triton X-100 for 1 hour at 4°C. The samples were subjected to ultracentrifugation at 50,000 g for 1 hour and incubated with pre-washed EZ View red anti-HA beads (Sigma) at 4°C for 3 hours. Protein-bead complexes were pelleted by centrifugation, washed 3 times in 1 ml 1% Triton X solution, and the proteins eluted from the beads using 100 µg/ml of the anti-HA antibody peptide before analysis by SDS PAGE and western blotting.

Isolation of T cells

A homogenous population of T cells were obtained from spleen tissue of WT or Glaxo P2X7^{-/-} mice following the protocol described in Okkenhaug et al. with slight modifications (Okkenhaug et al., 2006). Spleen tissue (WT and P2X7^{-/-}) was disrupted and the cellular suspension was pooled and subjected to T-cell isolation (~10⁸ cells/tissue). Total T cells were isolated by negative selection using FITC-conjugated anti-CD8, anti-CD69, anti-B220, anti-CD49b and anti-MHC class II antibodies (BD or eBioscience), followed by immunoprecipitation with anti-FITC MACS beads (Miltenyi Biotec), filtration and centrifugation. Cellular pellets were resuspended and analyzed by SDS-PAGE followed by western blot with anti-P2X7 antibody (Alomone).

Immunostaining

Immunostaining was carried out essentially as described previously (Guo et al., 2007).

In situ proximity ligation assay

In situ proximity ligation was carried out essentially as described previously using the Duolink 1 kit (Olink Bioscience) (Antonio et al., 2011). HEK293 cells were co-transfected with DNA encoding HA-tagged hPANX1 (hPANX1-HA) plus one of the following rat P2X receptor subtypes: P2X7, P2X2 or P2X4, along with pEGFP to identify transfected cells. The primary antibodies used were anti-HA, anti-P2X7-CT, anti-P2X2 and anti-P2X4, all diluted 1:100 in FBS plus saponin.

Electrophysiology

Whole-cell patch clamp recordings were carried out as described previously (Qureshi et al., 2007). The pipette solution was: 151 mM CsCl, 10 mM HEPES, 10 mM EGTA, 3 mM MgCl₂. Cells were maintained in normal extracellular solution (NES: 140 mM NaCl, 5 mM KCl, 2 mM CaCl₂, 1 mM MgCl₂, 10 mM D-glucose, 10 mM HEPES, pH 7.3). Voltage ramps of 1 s duration between -80 mV and +80 mV were applied at 5 s intervals. Hypotonic shock was applied by exchanging the isotonic NES (290 mOsm/l) with hypotonic NES (190 mOsm/l) made by diluting isotonic NES with H₂O. Pharmacological inhibitors of PANX1 currents were present in both isotonic and hypotonic saline at the concentrations indicated.

Dye uptake

Cells on glass coverslips were mounted on a suitable chamber and maintained in either NES or a low divalent NES (151 mM NaCl, 0.3 mM CaCl₂, 10 mM D-glucose, 10 mM HEPES, pH 7.3). Experiments to generate concentration-response relationships were performed in low divalent NES to improve the sensitivity of the measurements at low agonist concentrations (Fig. 1; Fig. 2E; Fig. 5G), whereas all other experiments were performed in NES as this contains more physiologically relevant levels of Ca²⁺, which might affect downstream signalling pathways. Apart from the shift in sensitivity to agonist there was essentially no difference in the results with either solution. The chamber was placed on the stage of a confocal microscope and imaging was carried out under 40× oil immersion objective at room temperature. Ethidium bromide (20 µM in NES), and BzATP were added to the cells at the specified time points in the presence or absence of drugs. Ethidium was excited at 543 nm and the emission light was collected at wavelengths ≥560 nm selected with a long-pass filter. The time course of dye uptake was recorded using LSM510 software (Zeiss). For analysis, the nuclear region for each cell was defined and the mean fluorescence intensity of the area was quantified and plotted as a function of time. Rate of uptake was calculated using data collected between 15 and 35 s after agonist application for BzATP-stimulated response and between 30 and 100 s for NAD-stimulated response. The maximal amplitude was less reliable because in some cells, highly expressing the receptor, there was some saturation of the signal at the end of the experiment. When constructing the BzATP concentration-response curves, the constitutive rate of dye uptake following the addition of ethidium, was subtracted from the rate measured post BzATP application, prior to normalization to the response to 100 µM BzATP at P2X7k, obtained on the same day. Hypotonic-shock-induced dye uptake was measured by initially maintaining cells in NES, applying ethidium bromide (20 µM) 25 s after starting the recording and then applying a hypotonic shock by adding a volume of H₂O to the cells that reduced the osmolarity of the solution from 290 mOsm/l to 190 mOsm/l.

[Ca²⁺]_i imaging

HEK cells expressing the P2X7a or P2X7k receptors were pre-incubated with 6 µM Fura-Red for 15 min at 37°C in DMEM. The cells were then washed once in NES and placed in a confocal chamber with NES. Cells were excited at 488 nm and emission collected between 505–550 nm with a band-pass filter. Changes in [Ca²⁺]_i following agonist application were measured as a drop in fluorescence due to the intracellular Fura-Red binding to free Ca²⁺.

Data analysis

Graphs were generated using Excel software (Microsoft) and statistical analysis was performed using unpaired *t*-test. Where applicable, standard error mean represented by error bars were indicated. Dose-response curves were generated using Prism 5 and the non-linear regression curve fit equation.

Funding

This work was supported by the Biotechnology and Biological Sciences Research Council [grant number BB/F001320/1 to R.D.M.-L.]; the Overseas Research Studentship [to X.J.X.]; the Cambridge Overseas Trust [to X.J.X.]; King's College Cambridge [to X.J.X.]; the Algerian government [to M. B.]; the David James studentship from the Department of Pharmacology, University of Cambridge [to L. R.]; the Fullbright Commission [to D.C.]; and the Transchannel Neuroscience Network (TC2N), EU Interreg Program [grant number 7-003-FR_TC2N to D.C.].

Supplementary material available online at

<http://jcs.biologists.org/lookup/suppl/doi:10.1242/jcs.099374/-/DC1>

References

- Adinolfi, E., Callegari, M. G., Ferrari, D., Bolognesi, C., Minelli, M., Wieckowski, M. R., Pinton, P., Rizzuto, R. and Di Virgilio, F. (2005). Basal activation of the P2X7 ATP receptor elevates mitochondrial calcium and potential, increases cellular ATP levels, and promotes serum-independent growth. *Mol. Biol. Cell* **16**, 3260-3272.
- Adinolfi, E., Cirillo, M., Woltersdorf, R., Falzoni, S., Chiozzi, P., Pellegatti, P., Callegari, M. G., Sandonà, D., Markwardt, F., Schmalzing, G. et al. (2010). Trophic activity of a naturally occurring truncated isoform of the P2X7 receptor. *FASEB J.* **24**, 3393-3404.
- Adriouch, S., Dox, C., Welge, V., Seman, M., Koch-Nolte, F. and Haag, F. (2002). Cutting edge: a natural P451L mutation in the cytoplasmic domain impairs the function of the mouse P2X7 receptor. *J. Immunol.* **169**, 4108-4112.
- Adriouch, S., Bannas, P., Schwarz, N., Fliegert, R., Guse, A. H., Seman, M., Haag, F. and Koch-Nolte, F. (2008). ADP-ribosylation at R125 gates the P2X7 ion channel by presenting a covalent ligand to its nucleotide binding site. *FASEB J.* **22**, 861-869.
- Antonio, L. S., Stewart, A. P., Xu, X. J., Varanda, W. A., Murrell-Lagnado, R. D. and Edwardson, J. M. (2011). P2X4 receptors interact with both P2X2 and P2X7 receptors in the form of homotrimeric. *Br. J. Pharmacol.* **163**, 1069-1077.
- Bao, L., Locovei, S. and Dahl, G. (2004). Pannexin membrane channels are mechanosensitive conduits for ATP. *FEBS Lett.* **572**, 65-68.
- Baranov, A., Ivanov, D., Petrash, N., Pestova, A., Skoblov, M., Kelmanson, L., Shagin, D., Nazarenko, S., Geraymovych, E., Litvin, O. et al. (2004). The mammalian pannexin family is homologous to the invertebrate innexin gap junction proteins. *Genomics* **83**, 706-716.
- Boumechache, M., Masin, M., Edwardson, J. M., Górecki, D. C. and Murrell-Lagnado, R. (2009). Analysis of assembly and trafficking of native P2X4 and P2X7 receptor complexes in rodent immune cells. *J. Biol. Chem.* **284**, 13446-13454.
- Brough, D., Le Feuvre, R. A., Iwakura, Y. and Rothwell, N. J. (2002). Purinergic (P2X7) receptor activation of microglia induces cell death via an interleukin-1-independent mechanism. *Mol. Cell. Neurosci.* **19**, 272-280.
- Cabrini, G., Falzoni, S., Forchap, S. L., Pellegatti, P., Balboni, A., Agostini, P., Cuneo, A., Castoldi, G., Baricordi, O. R. and Di Virgilio, F. (2005). A His-155 to Tyr polymorphism confers gain-of-function to the human P2X7 receptor of human leukemic lymphocytes. *J. Immunol.* **175**, 82-89.
- Cankurtaran-Sayar, S., Sayar, K. and Ugur, M. (2009). P2X7 receptor activates multiple selective dye-permeation pathways in RAW 264.7 and human embryonic kidney 293 cells. *Mol. Pharmacol.* **76**, 1323-1332.
- Cheewatrakoolpong, B., Gilchrist, H., Anthes, J. C. and Greenfeder, S. (2005). Identification and characterization of splice variants of the human P2X7 ATP channel. *Biochem. Biophys. Res. Commun.* **332**, 17-27.
- Chekeni, F. B., Elliott, M. R., Sandilos, J. K., Walk, S. F., Kinchen, J. M., Lazarowski, E. R., Armstrong, A. J., Penuela, S., Laird, D. W., Salvesen, G. S. et al. (2010). Pannexin 1 channels mediate 'find-me' signal release and membrane permeability during apoptosis. *Nature* **467**, 863-867.
- Chen, L. and Brosnan, C. F. (2006). Regulation of immune response by P2X7 receptor. *Crit. Rev. Immunol.* **26**, 499-513.
- Chessell, I. P., Hatcher, J. P., Bountra, C., Michel, A. D., Hughes, J. P., Green, P., Egerton, J., Murfin, M., Richardson, J., Peck, W. L. et al. (2005). Disruption of the P2X7 purinoceptor gene abolishes chronic inflammatory and neuropathic pain. *Pain* **114**, 386-396.
- Dardano, A., Falzoni, S., Caraccio, N., Polini, A., Tognini, S., Solini, A., Berti, P., Di Virgilio, F. and Monzani, F. (2009). 1513A>C polymorphism in the P2X7 receptor gene in patients with papillary thyroid cancer: correlation with histological variants and clinical parameters. *J. Clin. Endocrinol. Metab.* **94**, 695-698.
- Denlinger, L. C., Fiset, P. L., Sommer, J. A., Watters, J. J., Prabhu, U., DUBYAK, G. R., Proctor, R. A. and Bertics, P. J. (2001). Cutting edge: the nucleotide receptor P2X7 contains multiple protein- and lipid-interaction motifs including a potential binding site for bacterial lipopolysaccharide. *J. Immunol.* **167**, 1871-1876.
- Di Virgilio, F., Chiozzi, P., Ferrari, D., Falzoni, S., Sanz, J. M., Morelli, A., Torboli, M., Bolognesi, G. and Baricordi, O. R. (2001). Nucleotide receptors: an emerging family of regulatory molecules in blood cells. *Blood* **97**, 587-600.
- Donnelly-Roberts, D. L. and Jarvis, M. F. (2007). Discovery of P2X7 receptor-selective antagonists offers new insights into P2X7 receptor function and indicates a role in chronic pain states. *Br. J. Pharmacol.* **151**, 571-579.
- Eickhorst, A. N., Berson, A., Cockayne, D., Lester, H. A. and Khakh, B. S. (2002). Control of P2X(2) channel permeability by the cytosolic domain. *J. Gen. Physiol.* **120**, 119-131.
- Faria, R. X., Defarias, F. P. and Alves, L. A. (2005). Are second messengers crucial for opening the pore associated with P2X7 receptor? *Am. J. Physiol. Cell Physiol.* **288**, C260-C271.
- Feng, Y. H., Li, X., Wang, L., Zhou, L. and Gorodeski, G. I. (2006a). A truncated P2X7 receptor variant (P2X7-j) endogenously expressed in cervical cancer cells antagonizes the full-length P2X7 receptor through hetero-oligomerization. *J. Biol. Chem.* **281**, 17228-17237.
- Feng, Y. H., Li, X., Zeng, R. and Gorodeski, G. I. (2006b). Endogenously expressed truncated P2X7 receptor lacking the C-terminus is preferentially upregulated in epithelial cancer cells and fails to mediate ligand-induced pore formation and apoptosis. *Nucleosides Nucleotides Nucleic Acids* **25**, 1271-1276.
- Gu, B. J., Zhang, W., Worthington, R. A., Sluyter, R., Dao-Ung, P., Petrou, S., Barden, J. A. and Wiley, J. S. (2001). A Glu-496 to Ala polymorphism leads to loss of function of the human P2X7 receptor. *J. Biol. Chem.* **276**, 11135-11142.
- Gu, B. J., Rathsam, C., Stokes, L., McGeachie, A. B. and Wiley, J. S. (2009). Extracellular ATP dissociates nonmuscle myosin from P2X(7) complex: this dissociation regulates P2X(7) pore formation. *Am. J. Physiol. Cell Physiol.* **297**, C430-C439.
- Guerra, A. N., Fiset, P. L., Pfeiffer, Z. A., Quinchia-Rios, B. H., Prabhu, U., Aga, M., Denlinger, L. C., Guadarrama, A. G., Abozeid, S., Sommer, J. A. et al. (2003). Purinergic receptor regulation of LPS-induced signaling and pathophysiology. *J. Endotoxin Res.* **9**, 256-263.
- Guo, C., Masin, M., Qureshi, O. S. and Murrell-Lagnado, R. D. (2007). Evidence for functional P2X4/P2X7 heteromeric receptors. *Mol. Pharmacol.* **72**, 1447-1456.
- Hong, S., Schwarz, N., Brass, A., Seman, M., Haag, F., Koch-Nolte, F., Schilling, W. P. and DUBYAK, G. R. (2009). Differential regulation of P2X7 receptor activation by extracellular nicotinamide adenine dinucleotide and ecto-ADP-ribosyltransferases in murine macrophages and T cells. *J. Immunol.* **183**, 578-592.
- Iglesias, R., Locovei, S., Roque, A., Alberto, A. P., Dahl, G., Spray, D. C. and Semes, E. (2008). P2X7 receptor-Pannexin1 complex: pharmacology and signaling. *Am. J. Physiol. Cell Physiol.* **295**, C752-C760.
- Jiang, L. H., Rassendren, F., Mackenzie, A., Zhang, Y. H., Surprenant, A. and North, R. A. (2005). N-methyl-D-glucamine and propidium dyes utilize different permeation pathways at rat P2X(7) receptors. *Am. J. Physiol. Cell Physiol.* **289**, C1295-C1302.
- Khakh, B. S., Bao, X. R., Labarca, C. and Lester, H. A. (1999). Neuronal P2X transmitter-gated cation channels change their ion selectivity in seconds. *Nat. Neurosci.* **2**, 322-330.
- Kim, M., Jiang, L. H., Wilson, H. L., North, R. A. and Surprenant, A. (2001). Proteomic and functional evidence for a P2X7 receptor signalling complex. *EMBO J.* **20**, 6347-6358.
- Le Stunff, H., Auger, R., Kanellopoulos, J. and Raymond, M.-N. (2004). The Pro-451 to Leu polymorphism within the C-terminal tail of P2X7 receptor impairs cell death but not phospholipase D activation in murine thymocytes. *J. Biol. Chem.* **279**, 16918-16926.
- Locovei, S., Bao, L. and Dahl, G. (2006). Pannexin 1 in erythrocytes: function without a gap. *Proc. Natl. Acad. Sci. USA* **103**, 7655-7659.
- Locovei, S., Semes, E., Qiu, F., Spray, D. C. and Dahl, G. (2007). Pannexin1 is part of the pore forming unit of the P2X(7) receptor death complex. *FEBS Lett.* **581**, 483-488.
- Ma, W., Hui, H., Pelegrin, P. and Surprenant, A. (2009). Pharmacological characterization of pannexin-1 currents expressed in mammalian cells. *J. Pharmacol. Exp. Ther.* **328**, 409-418.
- Mackenzie, A. B., Young, M. T., Adinolfi, E. and Surprenant, A. (2005). Pseudoapoptosis induced by brief activation of ATP-gated P2X7 receptors. *J. Biol. Chem.* **280**, 33968-33976.
- Masin, M., Young, C., Lim, K., Barnes, S. J., Xu, X. J., Marschall, V., Brutkowski, W., Mooney, E. R., Górecki, D. C. and Murrell-Lagnado, R. (2012). Expression, assembly and function of novel C-terminal truncated variants of the mouse P2X7 receptor: re-evaluation of P2X7 knockouts. *Br. J. Pharmacol.* **165**, 978-993.
- Moore, S. F. and Mackenzie, A. B. (2007). Murine macrophage P2X7 receptors support rapid prothrombotic responses. *Cell. Signal.* **19**, 855-866.
- Nicke, A., Kuan, Y. H., Masin, M., Rettinger, J., Marquez-Klaka, B., Bender, O., Górecki, D. C., Murrell-Lagnado, R. D. and Soto, F. (2009). A functional P2X7 splice variant with an alternative transmembrane domain 1 escapes gene inactivation in P2X7 knock-out mice. *J. Biol. Chem.* **284**, 25813-25822.
- North, R. A. (2002). Molecular physiology of P2X receptors. *Physiol. Rev.* **82**, 1013-1067.
- Nuttall, L. C. and DUBYAK, G. R. (1994). Differential activation of cation channels and non-selective pores by macrophage P2z purinergic receptors expressed in *Xenopus* oocytes. *J. Biol. Chem.* **269**, 13988-13996.
- Okkenhaug, K., Patton, D. T., Bilancio, A., Garçon, F., Rowan, W. C. and Vanhaesebroeck, B. (2006). The p110delta isoform of phosphoinositide 3-kinase controls clonal expansion and differentiation of Th cells. *J. Immunol.* **177**, 5122-5128.
- Pelegrin, P. and Surprenant, A. (2006). Pannexin-1 mediates large pore formation and interleukin-1beta release by the ATP-gated P2X7 receptor. *EMBO J.* **25**, 5071-5082.
- Pelegrin, P. and Surprenant, A. (2009). The P2X(7) receptor-pannexin connection to dye uptake and IL-1beta release. *Purinergic Signal.* **5**, 129-137.
- Pfeiffer, Z. A., Aga, M., Prabhu, U., Watters, J. J., Hall, D. J. and Bertics, P. J. (2004). The nucleotide receptor P2X7 mediates actin reorganization and membrane blebbing in RAW 264.7 macrophages via p38 MAP kinase and Rho. *J. Leukoc. Biol.* **75**, 1173-1182.
- Placido, R., Auricchio, G., Falzoni, S., Battistini, L., Colizzi, V., Brunetti, E., Di Virgilio, F. and Mancino, G. (2006). P2X(7) purinergic receptors and extracellular ATP mediate apoptosis of human monocytes/macrophages infected with *Mycobacterium tuberculosis* reducing the intracellular bacterial viability. *Cell. Immunol.* **244**, 10-18.
- Qiu, F. and Dahl, G. (2009). A permeant regulating its permeation pore: inhibition of pannexin 1 channels by ATP. *Am. J. Physiol. Cell Physiol.* **296**, C250-C255.
- Qu, Y., Misaghi, S., Newton, K., Gilmour, L. L., Louie, S., Cupp, J. E., DUBYAK, G. R., Hackos, D. and Dixit, V. M. (2011). Pannexin-1 is required for ATP release during apoptosis but not for inflammasome activation. *J. Immunol.* **186**, 6553-6561.
- Qureshi, O. S., Paramasivam, A., Yu, J. C. and Murrell-Lagnado, R. D. (2007). Regulation of P2X4 receptors by lysosomal targeting, glycane protection and exocytosis. *J. Cell Sci.* **120**, 3838-3849.
- Ransford, G. A., Fregien, N., Qiu, F., Dahl, G., Conner, G. E. and Salathe, M. (2009). Pannexin 1 contributes to ATP release in airway epithelia. *Am. J. Respir. Cell Mol. Biol.* **41**, 525-534.

- Scemes, E., Spray, D. C. and Meda, P. (2009). Connexins, pannexins, innexins: novel roles of "hemi-channels". *Pflugers Arch.* **457**, 1207-1226.
- Schachter, J., Motta, A. P., de Souza Zamorano, A., da Silva-Souza, H. A., Guimarães, M. Z. and Persechini, P. M. (2008). ATP-induced P2X7-associated uptake of large molecules involves distinct mechanisms for cations and anions in macrophages. *J. Cell Sci.* **121**, 3261-3270.
- Seman, M., Adriouch, S., Scheuplein, F., Krebs, C., Freese, D., Glowacki, G., Deterre, P., Haag, F. and Koch-Nolte, F. (2003). NAD-induced T cell death: ADP-ribosylation of cell surface proteins by ART2 activates the cytolytic P2X7 purinoceptor. *Immunity* **19**, 571-582.
- Sikora, A., Liu, J., Brosnan, C., Buell, G., Chessel, I. and Bloom, B. R. (1999). Cutting edge: purinergic signaling regulates radical-mediated bacterial killing mechanisms in macrophages through a P2X7-independent mechanism. *J. Immunol.* **163**, 558-561.
- Smart, M. L., Gu, B., Panchal, R. G., Wiley, J., Cromer, B., Williams, D. A. and Petrou, S. (2003). P2X7 receptor cell surface expression and cytolytic pore formation are regulated by a distal C-terminal region. *J. Biol. Chem.* **278**, 8853-8860.
- Taylor, S. R., Gonzalez-Begne, M., Dewhurst, S., Chimini, G., Higgins, C. F., Melvin, J. E. and Elliott, J. I. (2008). Sequential shrinkage and swelling underlie P2X7-stimulated lymphocyte phosphatidylserine exposure and death. *J. Immunol.* **180**, 300-308.
- Taylor, S. R., Gonzalez-Begne, M., Sojka, D. K., Richardson, J. C., Sheardown, S. A., Harrison, S. M., Pusey, C. D., Tam, F. W. and Elliott, J. I. (2009). Lymphocytes from P2X7-deficient mice exhibit enhanced P2X7 responses. *J. Leukoc. Biol.* **85**, 978-986.
- Verhoef, P. A., Estacion, M., Schilling, W. and Dubyak, G. R. (2003). P2X7 receptor-dependent blebbing and the activation of Rho-effector kinases, caspases, and IL-1 beta release. *J. Immunol.* **170**, 5728-5738.
- Virginio, C., MacKenzie, A., North, R. A. and Surprenant, A. (1999). Kinetics of cell lysis, dye uptake and permeability changes in cells expressing the rat P2X7 receptor. *J. Physiol.* **519**, 335-346.
- Wiley, J. S., Dao-Ung, L. P., Gu, B. J., Sluyter, R., Shemon, A. N., Li, C., Taper, J., Gallo, J. and Manoharan, A. (2002). A loss-of-function polymorphic mutation in the cytolytic P2X7 receptor gene and chronic lymphocytic leukaemia: a molecular study. *Lancet* **359**, 1114-1119.
- Wilson, H. L., Wilson, S. A., Surprenant, A. and North, R. A. (2002). Epithelial membrane proteins induce membrane blebbing and interact with the P2X7 receptor C terminus. *J. Biol. Chem.* **277**, 34017-34023.
- Yan, Z., Li, S., Liang, Z., Tomić, M. and Stojilkovic, S. S. (2008). The P2X7 receptor channel pore dilates under physiological ion conditions. *J. Gen. Physiol.* **132**, 563-573.
- Yip, L., Woehrle, T., Corriden, R., Hirsh, M., Chen, Y., Inoue, Y., Ferrari, V., Insel, P. A. and Junger, W. G. (2009). Autocrine regulation of T-cell activation by ATP release and P2X7 receptors. *FASEB J.* **23**, 1685-1693.